Guo *et al.*
Chinese Journal of Mechanical Engineering (2023) 36:135
https://doi.org/10.1186/s10033-023-00964-9

Chinese Journal of Mechanical Engineering

ORIGINAL ARTICLE

Open Access

A New Dynamics Analysis Model for Five-Axis Machining of Curved Surface Based on Dimension Reduction and Mapping

Minglong Guo[2], Zhaocheng Wei[1*], Minjie Wang[1], Zhiwei Zhao[1] and Shengxian Liu[1]

Abstract

The equipment used in various fields contains an increasing number of parts with curved surfaces of increasing size. Five-axis computer numerical control (CNC) milling is the main parts machining method, while dynamics analysis has always been a research hotspot. The cutting conditions determined by the cutter axis, tool path, and workpiece geometry are complex and changeable, which has made dynamics research a major challenge. For this reason, this paper introduces the innovative idea of applying dimension reduction and mapping to the five-axis machining of curved surfaces, and proposes an efficient dynamics analysis model. To simplify the research object, the cutter position points along the tool path were discretized into inclined plane five-axis machining. The cutter dip angle and feed deflection angle were used to define the spatial position relationship in five-axis machining. These were then taken as the new base variables to construct an abstract two-dimensional space and establish the mapping relationship between the cutter position point and space point sets to further simplify the dimensions of the research object. Based on the in-cut cutting edge solved by the space limitation method, the dynamics of the inclined plane five-axis machining unit were studied, and the results were uniformly stored in the abstract space to produce a database. Finally, the prediction of the milling force and vibration state along the tool path became a data extraction process that significantly improved efficiency. Two experiments were also conducted which proved the accuracy and efficiency of the proposed dynamics analysis model. This study has great potential for the online synchronization of intelligent machining of large surfaces.

Keywords Curved surface, Five-axis machining, Dimension reduction and mapping, Milling force, Dynamics

1 Introduction

Parts with curved surfaces that can effectively meet the demands of equipment function, efficiency, and personalization are increasingly used in the fields of home appliances, automobiles, energy, and aviation. Computer numerical control (CNC) machining is the main machining method for these types of parts because of advantages such as high precision and high efficiency. In five-axis machining, the process, tool path, and cutter-axis planning are flexible with lower clamping times and higher efficiency and precision, which have become a trend in the development of CNC machining technology in the future. CNC milling dynamics has long been a hot but and difficult research topic, among which the cutting force and vibration state play a key role in machining deformation, cutter wear, machining efficiency, surface quality, production cost, and even safety. Dynamics analysis mainly focuses on the cutter-workpiece contact geometry and the vibration differential equation, and the results of related research are remarkable. However, with

*Correspondence:
Zhaocheng Wei
wei_zhaocheng@dlut.edu.cn
[1] Key Laboratory for Precision and Non-traditional Machining Technology of Ministry of Education, Dalian University of Technology, Dalian 116024, People's Republic of China
[2] Institute of Mechanical Manufacturing Technology, China Academy of Engineering Physics, Mianyang 621000, China

the increasing size and complexity of curved surfaces, the problems of high complexity, large amount of computation, and low efficiency of traditional research methods for cutter-workpiece contact geometry and vibration differential equation have emerged, making it difficult to meet the practical application requirements of dynamics theory.

The dynamics modeling of simple geometric workpieces is easy, such as the three-axis machining of a horizontal plane, an inclined plane, and a cylindrical surface [1–3]. Even if the inclined plane is machined by five axes, the analytical method can be used for modeling [4]. For the five-axis machining of a curved surface, the arbitrariness of the cutter axis and tool path increases the difficulty of dynamics modeling, which is mainly reflected in the contact solution between the workpiece and the cutting edge. The contact constantly changes in the time domain and must be calculated in real time. The first method for contact solution is a solid modeling method. Based on the modeling function of 3D software, a Boolean intersection operation is performed on the cutter swept body and part entity to extract the actual contact information [5]. The development cost of solid modeling is high, the amount of operation process data is huge, and the efficiency is low. Therefore, Yang et al. [6] used the possible contact surface to trim the swept surface. Ferri et al. [7] discretized the removed body into thin layers. Boz et al. [8] discretized the cutter into independent cutting thin layers. All the above studies optimized the solid modeling method and improved the efficiency by varying degrees. The second method is the discrete method represented by Z-Map, which uses point vectors to describe the workpiece body, and analyzes the contact by calculating the position of the cutting-edge element relative to the workpiece along the vector [9]. Wei et al. [10] introduced a logical array identification function. Aras et al. [11] described a new parametric method to update the workpiece surface, which further improved the efficiency of the discrete method. The third method is an analytical method that uses mathematical formulas to describe the contact. Sun et al. [12] established a bounding box using the unmachined surface, the machined surface, and the swept surface of the cutting edge to analyze and judge the cutter-workpiece contact. Zhang et al. [13] analytically solved the cutting-out and cutting-in of the cutting edge with a boundary curve equation of the rectangular contact region for the side milling of a flat-end mill. In summary, the efficiency of the analytical, discrete, and solid methods to analyze the contact geometry in the five-axis machining of curved surfaces decreases in turn, and are all based on known curved surfaces. In the face of an extremely long CNC tool path on a large curved surface, it is difficult to perform real-time calculations of the cutter-workpiece contact in each instantaneous state even if the analytical method is used. This results in a low-efficiency dynamics model and makes intelligent online prediction impossible.

Dynamics analysis considers the cutting force to determine the self-excited vibration state of the machining system. At present, the classic methods of dynamics analysis include the single-frequency method [14], the multifrequency method [15], the time-domain finite simulation method [16] and the discrete method [17–19]. The experimental method [20] directly obtains the machining state signal through a sensor, which is commonly used to support other stability prediction theories. However, few studies have been conducted on the dynamics of the five-axis milling of a curved surface. Taking the five-axis machining of a blisk as the research object, and considering the effect of material removal during the machining process, Budak et al. [21] used a finite element model of the workpiece to describe the changes of the dynamic parameters in the cutting position, and established a vibration theoretical model. Ozkirimli et al. [22] established a dynamics model for the multi-axis milling of a curved surface with general geometric cutters. Based on the zero-order single-frequency method, they obtained a machining stability limit diagram. Ozturk et al. [23] carried out chatter stability analysis based on the frequency-domain method, time-domain method, and experimental method for five-axis machining. They concluded that the multifrequency effect has a significant influence on machining stability. The complete discretization method is currently the most accurate for chatter stability analysis, but requires a large number of calculations [19]. The dynamics modeling of a curved surface in five-axis machining is currently too complex for the use of a complete discrete method in chatter stability analysis. Therefore, the dynamics analysis model must be further improved in terms of efficiency and accuracy.

The concept of differential discretization has been applied in various engineering fields, machining, and manufacturing. The most common application is the discretization of the cutting edge into a series of tiny straight-edge segments [24]. To calculate the cutting thickness, the simultaneous motion of the cutter feed and rotation is discretized into independent alternating motions [24]. Boz et al. [8] discretized the cutter into thin layers during cutter-workpiece contact analysis. The vector representation of a workpiece is also a discrete application [9]. The unit of research in chatter stability analysis with the complete discretization method is also a tiny time interval [19]. In CNC machining, the tool path is a curve consisting of broken line segments connected from end to end. Similarly, the curved surface can be approximately discretized into interconnected inclined

planes. Wei et al. [25] transformed the research object from a curved surface into an inclined plane, which laid the foundation for the work in this paper.

To deal with the abovementioned problems in the five-axis CNC machining of a curved surface, this paper introduces the idea of dimension reduction and mapping, and proposes a new dynamics analysis model. The two main innovations of this study are as follows. (1) Through the discrete expression of the tool path and the extraction of new base variables, an abstract two-dimensional space with a mapping relationship between the cutter position points in the five-axis machining of a curved surface is constructed. (2) The dynamics of an inclined plane five-axis machining unit is studied, and the results are stored in the abstract space to produce a database that will transform the prediction of the milling force and vibration state in five-axis machining into a simple and fast data extraction process.

2 Differential Discretization in CNC Machining

2.1 Characteristics of Machining Parameters

In the CNC machining process, the profile of parts obtained after rough machining has a uniform allowance layer to be machined. The machining allowance in the subsequent semi-finishing and finishing machining process, i.e., the normal cutting depth d_n, remains unchanged. As shown in Figure 1, when the existing CAM machining programming module plans the tool path for semi-finishing and finishing machining to stabilize and smoothen the cutting load, the step distance s, rotational speed w, and feed rate f_v can only be set to a certain fixed value, and the machining process remains unchanged from beginning to end. In contrast, to adapt to the geometric profile of complex parts and consider the requirements of cutter-axis interference, surface roughness, and residual materials, the feed direction $\boldsymbol{f}$ along the tool path and cutter axis vector $\boldsymbol{p}$ are arbitrary and changeable. Among them, the common following periphery, reciprocating and circular tool path strategies are shown in Figure 1.

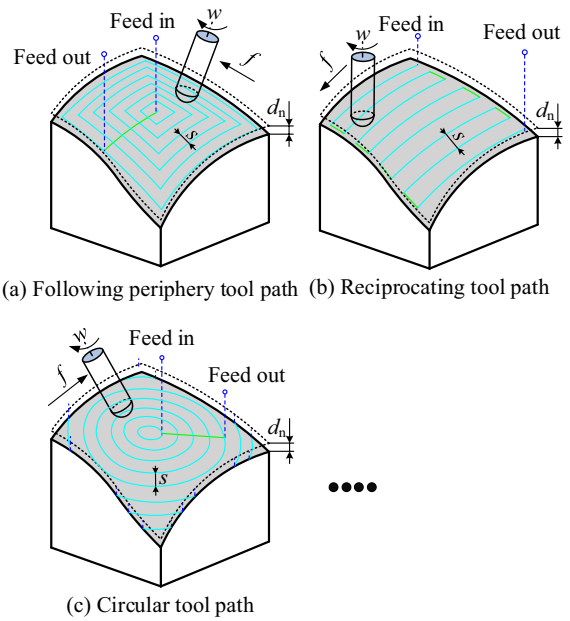

Figure 1 Machining parameters in five-axis machining of curved surfaces

2.2 Cutter Position Points Analysis along Tool Path

As shown in Figure 2(a), using the concept of differential discretization, the interpolated straight lines can be directly used to discretize the tool path with each endpoint of the line segment as a cutter position point. Based on differential discretization again, any curved surface is considered to be a combination of countless micro-inclined planes. Therefore, curved surface machining can be further approximated as inclined plane machining at a discrete cutter position point. The cutter moves in a straight line from one position to the next along the tool path. The feed direction $\boldsymbol{f}$ in inclined plane machining

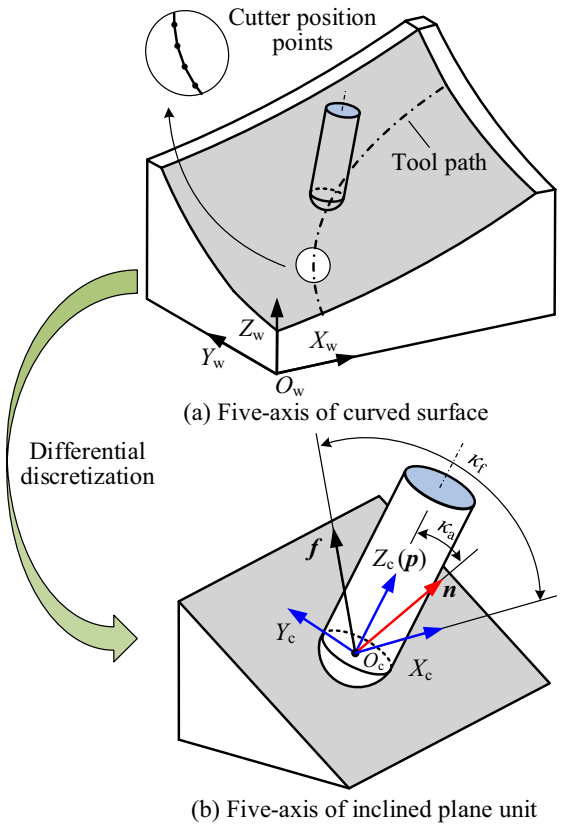

Figure 2 Five-axis machining of a curved surface

is the vector of two consecutive cutter positions, and is located in the inclined plane. The normal direction $\boldsymbol{n}$ of the curved surface is used to define the inclined plane at the cutter position point.

As shown in Figure 2(b), the cutter coordinate system O_c-$X_cY_cZ_c$ obeys the right-hand rule. The origin O_c is the sphere center of the ball-end mill. The Z_c-axis is upward along the central axis of the milling cutter. The cross-product vector of the cutter axis $\boldsymbol{p}$ and workpiece normal $\boldsymbol{n}$ is taken as the X_c-axis.

In O_c-$X_cY_cZ_c$, the feed deflection angle κ_f is the angle between the feed direction f and X_c-axis, as shown in Eq. (1). If the angle between the vector obtained by cross-multiplying the X_c-axis and feed direction and cutter axis $\boldsymbol{p}$ is less than 90 °, then the κ_f is positive; otherwise, it is negative.

$$\kappa_f = \arccos\left(\frac{(\boldsymbol{p}\times\boldsymbol{n})\cdot\boldsymbol{f}}{|\boldsymbol{p}\times\boldsymbol{n}||\boldsymbol{f}|}\right), \tag{1}$$

The cutter dip angle κ_a is the angle between the normal direction $\boldsymbol{n}$ and cutter axis $\boldsymbol{p}$, as shown in Eq. (2), which reflects the degree of inclination of the cutter axis relative to the workpiece.

$$\kappa_a = \arccos\left(\frac{\boldsymbol{n}\cdot\boldsymbol{p}}{|\boldsymbol{n}||\boldsymbol{p}|}\right). \tag{2}$$

In CAM software, the front rake and side rake angles are often used to define the cutter axis, which describes the relationship between the workpiece normal, feed direction, and cutter axis; but does not describe its relationship with the cutter coordinate system. In contrast, the three relationships defined in this study are more advantageous, scientific, and reasonable in five-axis machining research.

Differential discretization can transform the research object from a curved surface into a simple inclined plane and the cutting condition from a continuous nonconstant state into a series of transient constant states, which can significantly reduce the research complexity of the five-axis machining of curved surfaces.

3 Reducing Dimension and Mapping

3.1 Abstract Two-Dimensional Space

In the vector space R^m, if there are m vectors $\boldsymbol{x}_1$, $\boldsymbol{x}_2$, …, $\boldsymbol{x}_m$ satisfying linear independence, any vector $\boldsymbol{x}$ can be expressed linearly by these m vectors. The $\boldsymbol{x}_1$, $\boldsymbol{x}_2$, …, $\boldsymbol{x}_m$ are called a base of vector space R^m. The mathematical expression is as follows:

$$\mathbb{R}^m = \left\{\boldsymbol{x} = (\alpha_1\boldsymbol{x}_1+\alpha_2\boldsymbol{x}_2+\cdots+\alpha_m\boldsymbol{x}_m)^{\mathrm{T}} \mid \alpha_1,\alpha_2,\cdots,\alpha_m\in\mathbb{R}\right\}. \tag{3}$$

A vector space usually has more than one base. If $\boldsymbol{x}_1$, $\boldsymbol{x}_2$, …, $\boldsymbol{x}_m$ and $\boldsymbol{x}_1'$, $\boldsymbol{x}_2'$, …, $\boldsymbol{x}_m'$ are two bases in the linear space R^m, then the base transformation is

$$\begin{pmatrix}\boldsymbol{x}_1'\\ \boldsymbol{x}_2'\\ \vdots\\ \boldsymbol{x}_m'\end{pmatrix}^{\mathrm{T}} = \begin{pmatrix}\boldsymbol{x}_1\\ \boldsymbol{x}_2\\ \vdots\\ \boldsymbol{x}_m\end{pmatrix}^{\mathrm{T}} \begin{bmatrix}\alpha_{11} & \alpha_{12} & \cdots & \alpha_{1m}\\ \alpha_{21} & \alpha_{22} & \cdots & \alpha_{2m}\\ \vdots & \vdots & \ddots & \vdots\\ \alpha_{m1} & \alpha_{m2} & \cdots & \alpha_{mm}\end{bmatrix}. \tag{4}$$

Base transformation theory can study the same problem from different angles, and it is possible to obtain laws that are difficult to find and describe under the original base.

Based on differential discretization, the dynamics of inclined plane milling at the cutter position can be studied easily to obtain the force and vibration state of curved surface milling along the tool path. However, there are still two disadvantages. (1) The discrete processing requires a large amount of calculation and storage, which is possible for some small-scale surface workpieces. However, for large-scale surfaces, such as a compressor impeller and automobile panel mold, the tool path sampling points can reach millions or more, which the differential method cannot deal with. (2) The discretized results of single or multiple surfaces have a large number of tiny inclined plane machining processes with the same cutting conditions. The differential method is unable to reuse these repeated cutting processes as well as avoid repeated calculations, resulting in the waste of computing resources and increased costs.

Based on the mathematical idea of dimension reduction and mapping, the change law of cutting motion geometry can be analyzed and studied from the traditional Cartesian coordinate system to other spaces to simplify complex problems. As described in Section 2.2, the relationship between the cutter coordinate system, feed direction, cutter axis, and workpiece in five-axis machining can be accurately and uniquely described by the cutter dip angle and feed deflection angle. In this study, these two angles are new characteristic parameters used as base variables to establish a two-dimensional space.

3.2 Dynamics Analysis Process

In Figure 3(a), the tool path is sinusoidal, and the front rake and side rake angles for five-axis machining were set as 10° and 30°, respectively. In the abstract two-dimensional space in Figure 3(b), the series of cutter position points for three-axis machining correspond to point set

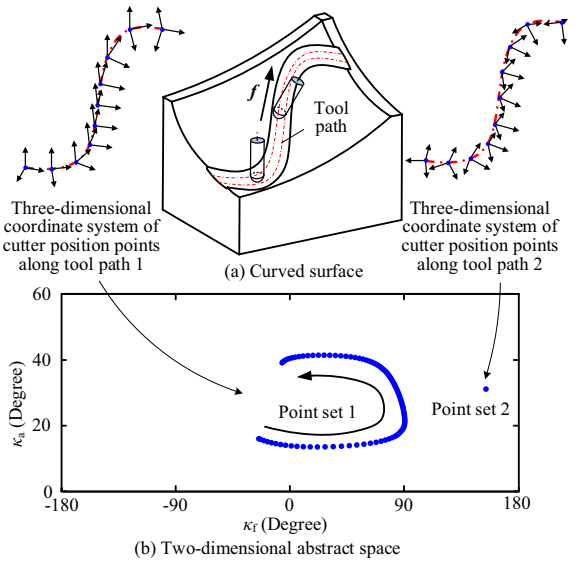

Figure 3 Mapping relationship of curved surface machining

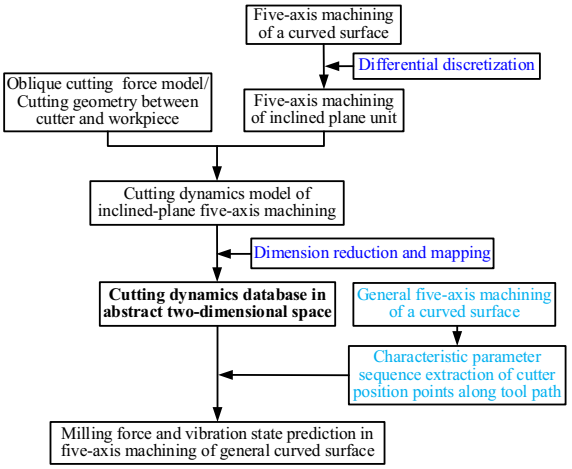

Figure 4 Dynamics analysis process based on dimension reduction and mapping

1. The feed deflection angle κ_f and cutter dip angle κ_a of each cutter position point are different. The corresponding point set 2 of the cutter position points for five-axis machining is only one point because each cutter position point has the same deflection angle κ_f and dip angle κ_a.

It is obvious that arbitrary inclined-plane five-axis machining can be represented by a point, while sequence inclined-plane machining corresponds to a set of points. By dimension reduction and mapping with the differential method, the cutter position points of the curved surface in five-axis machining correspond to the set of points. The problem of the five-axis machining of a curved surface in a traditional three-dimensional space is successfully transformed into a set of points in an abstract two-dimensional space, thus achieving the goal of dimensionality reduction and simplification.

Based on the cutting dynamics theory of an inclined-plane five-axis machining unit, the new base variable combinations are uniformly sampled, and the results are stored to produce an abstract dynamics database. For the general five-axis machining of a curved surface, dynamics analysis can be performed by searching the base variable sequence along the tool path. The detailed prediction process of static milling force and vibration state is shown in Figure 4. Among them, the abstract database is the link between the theoretical model and the practical application, making the prediction process into fast data extraction.

4 Dynamics Analysis Model

4.1 Dynamics Derivation of Inclined Plane

As shown in Figure 5(a), the ball-end mill is commonly used for the semi-finishing and finishing machining of a curved surface. Figure 5(b) is an independent straight-edge oblique cutting corresponding to the discrete element of the cutting edge. The cutting force element is calculated by combining the mechanical model of oblique cutting, actual machining parameters, and cutter geometry.

The cutting force element includes the shear and plough zones. Its radial component dF_r, tangential component dF_t, and axial component dF_a on the cutting edge j are expressed as

$$\begin{cases} dF_{r,j}(\theta,k) = K_{rc}t_c(\theta,k)db + K_{re}ds, \\ dF_{t,j}(\theta,k) = K_{tc}t_c(\theta,k)db + K_{te}ds, \\ dF_{a,j}(\theta,k) = K_{ac}t_c(\theta,k)db + K_{ae}ds, \end{cases} \tag{5}$$

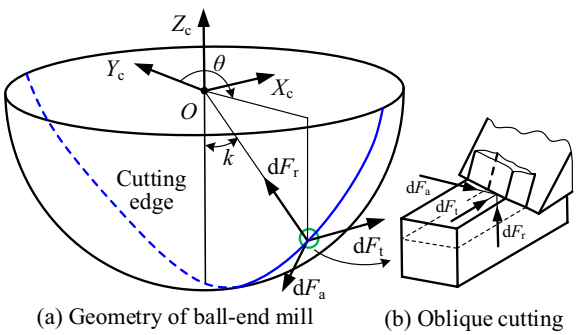

Figure 5 Force analysis of ball-end mill

where k and θ are the axial and radial position angles, respectively. t_c is the instantaneous cutting thickness [25]. ds and db are the cutting length and width, respectively. K_{rc}, K_{tc}, and K_{ac} are the shear force coefficients in the radial, tangential, and axial directions, respectively [25]. K_{re} and K_{te} are the radial and tangential plough force coefficients [26] expressed as Eqs. (11) and (12), respectively. The axial plough force coefficient K_{ae} is taken as zero [27].

$$\begin{cases} K_{rc}=K_{xs}\sin(\beta_n-\alpha_n)\cos\eta_i^{-1}, \\ K_{tc}=K_{xs}\tan\eta_i\tan\eta_f\sin\beta_n+\cos(\beta_n-\alpha_n), \\ K_{ac}=K_{xs}\cos(\beta_n-\alpha_n)\tan\eta_i-\tan\eta_f\sin\beta_n, \\ K_{xs}=\dfrac{\tau_s\sin\phi_n^{-1}}{\sqrt{\tan^2\eta_f\sin^2\beta_n+\cos^2(\phi_n+\beta_n-\alpha_n)}}, \end{cases} \tag{6}$$

$$\begin{cases} K_{re}=\{\cos(\phi_n-\gamma_p+\eta_p)[1+2\theta_p+2\gamma_p+\sin(2\eta_p)] \\ \quad -\sin(\phi_n-\gamma_p+\eta_p)\cos(2\eta_p)\}\tau_s r_p, \\ K_{te}=\{\sin(\phi_n-\gamma_p+\eta_p)[1+2\theta_p+2\gamma_p+\sin(2\eta_p)] \\ \quad +\cos(\phi_n-\gamma_p+\eta_p)\cos(2\eta_p)\}\sin\eta_p^{-1}\tau_s r_p, \end{cases} \tag{7}$$

where, ϕ_n, β_n, and α_n are the normal shear angle, friction angle, and forward angle, respectively. η_f is the chip outflow angle. η_i is the cutting-edge inclination angle. r_p and γ_p are the sector radius and angle of the slip line in the ploughing zone, respectively. η_p is the angle between the slip line and plough plane. θ_p is the sector angle of the slip line at the outer end of the shear zone. Comprehensively considering the dynamic mechanical properties and mesoscopic size effect of material cutting, the shear stress τ_s is expressed as follows [28]:

$$\tau_s=\tau_{JC}\left[\left(\frac{\tau_{JC}}{\alpha_t Gb}\right)^{2(u_2-u_1)}+\left(\frac{\tau_{JC}}{\alpha_t Gb}\right)^{-2u_1}\left(\frac{\overline{r}\overline{\eta}}{b}\right)^{u_3}\right]^{\frac{1}{2u_1}}, \tag{8}$$

where α_t is the stress constant coefficient, G is the shear modulus, b is the Burgers vector mode, $\overline{r}$ is the Nye factor, and $\overline{\eta}$ is the strain gradient in the shear zone. u_1, u_2, and u_3 are the dislocation density correction coefficients. τ_{JC} is the macroscopic plastic deformation shear stress reflecting the thermal softening, strain rate strengthening, and strain hardening effects during the plastic deformation process.

All the cutting force elements on N cutting edges are transformed into O_c-$X_cY_cZ_c$ and calculated cumulatively.

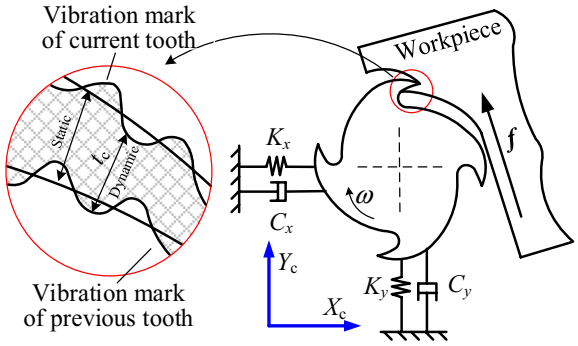

Figure 6 Self-excited vibration in milling system

Finally, the milling force components on the X_c-, Y_c-, and Z_c-axis at any cutter rotation angle are shown in Eq. (9).

$$\begin{bmatrix} F_{cx} \\ F_{cy} \\ F_{cz} \end{bmatrix}=\sum_{j=1}^{N}\int_{k_d}^{k_u}\left\{\begin{bmatrix} -\sin\theta\sin k & -\cos\theta & -\sin\theta\cos k \\ -\cos\theta\sin k & \sin\theta & -\cos\theta\cos k \\ \cos k & 0 & -\sin k \end{bmatrix}\begin{bmatrix} dF_{r,j} \\ dF_{t,j} \\ dF_{a,j} \end{bmatrix}\right\}, \tag{9}$$

where k_d and k_u are the lower and upper boundary points of the cutting-edge interval that participates in material cutting, respectively. The cutting edge element in O_c-$X_cY_cZ_c$ is converted into an auxiliary coordinate system, and the space limitation method is used to determine whether it participates in cutting. In the auxiliary coordinate system, the feed direction $\boldsymbol{f}$ is the Y_c-axis, and the normal direction $\boldsymbol{n}$ is the Z_c -axis; the other definitions are the same as O_c-$X_cY_cZ_c$. The conditions of the cutting-edge element coordinates (x y z) participating in the material cutting are shown in Eq. (15) [25].

$$\begin{cases} (x-s)^2+z^2>R^2, \\ y>0, \\ z+R-d_n<0. \end{cases} \tag{10}$$

The periodic fluctuations of the cutting force caused by the dynamic cutting thickness induced self-excited vibration. Based on the above static milling force, the dynamics model can be established to determine whether the machining system is stable or chattering. Most of the parts with large-scale surfaces are rigid. The flexible cutter milling system with two degrees-of-freedom is taken as an example, as shown in Figure 6.

The milling force is the sum of the products of the mass and acceleration, damping and velocity, and stiffness and displacement. The vibration differential equation in the X_c-axis and Y_c-axis directions is

$$\begin{bmatrix} M_x & 0 \\ 0 & M_y \end{bmatrix}\begin{bmatrix} \ddot{x}(t) \\ \ddot{y}(t) \end{bmatrix}+\begin{bmatrix} C_x & 0 \\ 0 & C_y \end{bmatrix}\begin{bmatrix} \dot{x}(t) \\ \dot{y}(t) \end{bmatrix}+\begin{bmatrix} K_x & 0 \\ 0 & K_y \end{bmatrix}\begin{bmatrix} x(t) \\ y(t) \end{bmatrix}=\boldsymbol{W}_c(t)\begin{bmatrix} x(t)-x(t-T) \\ y(t)-y(t-T) \end{bmatrix}+\boldsymbol{h_0}(t), \tag{11}$$

where $\boldsymbol{K}$, C, and $\boldsymbol{M}$ are the stiffness matrix, damping matrix, and mass matrix, respectively; these are isotropic, and coupling is ignored.

In Eq. (11), the right side is the dynamic milling force. The static term $h_0(t)$ is omitted, and only the milling force caused by the regeneration effect is considered.

$$\boldsymbol{W}_{\mathbf{c}}(t) = \sum_{j=1}^{N} \int_{k_{\mathrm{d},j}}^{k_{\mathrm{u},j}} \begin{bmatrix} W_{11} & W_{12} \\ W_{21} & W_{22} \end{bmatrix} \mathrm{d}k, \tag{12}$$

where the matrix elements are

$$\begin{cases} W_{11} = R\sin\theta\sin k(-K_{\mathrm{rc}}\sin k\sin\theta - K_{\mathrm{tc}}\cos\theta - K_{\mathrm{ac}}\cos k\sin\theta), \\ W_{12} = R\cos\theta\sin k(-K_{\mathrm{rc}}\sin k\sin\theta - K_{\mathrm{tc}}\cos\theta - K_{\mathrm{ac}}\cos k\sin\theta), \\ W_{21} = R\sin\theta\sin k(K_{\mathrm{rc}}\sin k\cos\theta - K_{\mathrm{tc}}\sin\theta - K_{\mathrm{ac}}\cos k\cos\theta), \\ W_{22} = R\cos\theta\sin k(K_{\mathrm{rc}}\sin k\cos\theta - K_{\mathrm{tc}}\sin\theta - K_{\mathrm{ac}}\cos k\cos\theta). \end{cases} \tag{13}$$

The complete discrete method is used for vibration state analysis [19]. The Euler form of the vibration differential equation is expressed as

$$\dot{\boldsymbol{u}}(t) = \boldsymbol{Q}(t)\boldsymbol{u}(t-T) + \boldsymbol{P}(t)\boldsymbol{u}(t), \tag{14}$$

where the vector $\boldsymbol{u}(t)$ is shown in Eq. (15). The dimensions of matrices $\boldsymbol{P}(t)$ and $\boldsymbol{Q}(t)$ are both 4×4, as shown in Eq. (16).

$$\boldsymbol{u}(t) = [x(t)\, y(t)\, \dot{x}(t)\, \dot{y}(t)]^{\mathrm{T}}, \tag{15}$$

$$\begin{cases} \boldsymbol{P}(t) = \begin{bmatrix} \boldsymbol{0} & \boldsymbol{I} \\ \boldsymbol{M}^{-1}\boldsymbol{W}_{\mathbf{c}}(t) - \boldsymbol{M}^{-1}\boldsymbol{K} & -\boldsymbol{M}^{-1}\boldsymbol{C} \end{bmatrix}, \\ \boldsymbol{Q}(t) = \begin{bmatrix} \boldsymbol{0} & \boldsymbol{0} \\ -\boldsymbol{M}^{-1}\boldsymbol{W}_{\mathbf{c}}(t) & \boldsymbol{0} \end{bmatrix}. \end{cases} \tag{16}$$

The time t is discretized into a series of continuous, tiny time intervals of length Δt. Let the cutting period $T = m\Delta t$, and m takes an integer. In Eq. (14), the periodic factor matrix is taken as the average value; the time-domain and time-delay terms are taken as linear interpolation; and the differential term is discretized by the forward difference quotient. The iteration equation in the pth time interval (t_p, t_{p+1}) is as follows:

$$\boldsymbol{v}_{p+1} = \boldsymbol{D}_p \boldsymbol{v}_p, \tag{17}$$

where v_p is a $4(m+1)$-dimensional state column vector, as in Eq. (18). D_p is a relation transformation matrix, as shown in Eq. (19).

$$\begin{aligned} \boldsymbol{v}_p = \mathrm{col}(&x_p, y_p, \dot{x}_p, \dot{y}_p \ldots x_{p-m+1}, \\ &y_{p-m+1}, \dot{x}_{p-m+1}, \dot{y}_{p-m+1}, \\ &x_{p-m}, y_{p-m}, \dot{x}_{p-m}, \dot{y}_{p-m}), \end{aligned} \tag{18}$$

$$\boldsymbol{D}_p = \begin{pmatrix} (\boldsymbol{I} - a_{\mathrm{i}}\boldsymbol{P}_p)^{-1}(\boldsymbol{I} + \Delta t\boldsymbol{P}_p - a_{\mathrm{i}}\boldsymbol{P}_p) & \boldsymbol{0}\ \boldsymbol{0}\ \ldots\ \boldsymbol{0} & (\boldsymbol{I} - a_{\mathrm{i}}\boldsymbol{P}_p)^{-1}a_{\mathrm{i}}\boldsymbol{Q}_p & (\boldsymbol{I} - a_{\mathrm{i}}\boldsymbol{P}_p)^{-1}(\Delta t - a_{\mathrm{i}})\boldsymbol{Q}_p \\ \boldsymbol{I} & \boldsymbol{0}\ \boldsymbol{0}\ \ldots\ \boldsymbol{0} & \boldsymbol{0} & \boldsymbol{0} \\ \boldsymbol{0} & \boldsymbol{I}\ \boldsymbol{0}\ \ldots\ \boldsymbol{0} & \boldsymbol{0} & \boldsymbol{0} \\ \vdots & \vdots\ \vdots\ \ddots\ \vdots & \vdots & \vdots \\ \boldsymbol{0} & \boldsymbol{0}\ \boldsymbol{0}\ \ldots\ \boldsymbol{0} & \boldsymbol{0} & \boldsymbol{0} \\ \boldsymbol{0} & \boldsymbol{0}\ \boldsymbol{0}\ \ldots\ \boldsymbol{I} & \boldsymbol{0} & \boldsymbol{0} \\ \boldsymbol{0} & \boldsymbol{0}\ \boldsymbol{0}\ \ldots\ \boldsymbol{0} & \boldsymbol{I} & \boldsymbol{0} \end{pmatrix}. \tag{19}$$

The state transition relationship within a single cutting cycle T is constructed as follows:

$$\boldsymbol{v}_m = \boldsymbol{\Phi}_{\mathbf{s}}\boldsymbol{v}_0, \tag{20}$$

where $\boldsymbol{\Phi}_{\mathrm{s}}$ is the transfer matrix:

$$\boldsymbol{\Phi}_{\mathbf{s}} = \boldsymbol{D}_{m-1}\boldsymbol{D}_{m-2}\cdot\cdots\cdot\boldsymbol{D}_1\boldsymbol{D}_0. \tag{21}$$

The vibration differential equation is linear with periodic coefficients. According to the Floquet theory, if the maximum modulus of all the eigenvalues of the transfer matrix Φ_{s} is less than 1, then the milling system is stable. If the maximum modulus is equal to 1, then the system is in a critical state. If there are modules greater than 1, then the system will be chattering.

Therefore, the dynamics (milling force and vibration) of inclined plane five-axis machining can be calculated under arbitrary conditions of the cutter axis, feed direction, and machining parameters (rotational speed, step distance, and cutting depth).

4.2 Abstract Dynamics Database

In the five-axis machining of a curved surface, the feed rate, cutting depth, step distance, and rotational speed remain unchanged during the operation of the CNC program, as described in Section 2.1. The tool path and cutter axis change with the workpiece geometry. Based on the above dynamics modeling of an inclined plane five-axis machining unit, the static milling force and vibration state under different combinations of the

cutter dip angle and feed deflection angle can be calculated, and the abstract two-dimensional dynamics database can be constructed.

Taking a cemented carbide ball-end mill as an example, the cutting edge is equal lead right-handed. The radius is 4 mm, the number of teeth is 4, the nominal helix angle is 30°, the blunt radius of the cutting edge is 5 μm, and the normal rake angle is 6°. A quenched and tempered 45 steel workpiece with a hardness of HRC33 is taken as an example. The thermodynamic characteristics are known [29]. The macroscopic plastic deformation shear stress τ_{JC} is expressed as Eq. (22) [29].

$$\tau_{JC}=\frac{1}{\sqrt{3}}\left[A(HRC)+244\varepsilon^{n(HRC)}\right]\left[1+0.0877\ln(\frac{\dot{\varepsilon}}{\dot{\varepsilon}_0})\right]\exp\left[-(\frac{T^*+0.005989}{0.4415})^2\right], \tag{22}$$

where A is the initial yield stress of the material. n is the strain-hardening index, expressed as Eq. (23). ε, $\dot{\varepsilon}$, and $\dot{\varepsilon}_0$ are the plastic strain, strain rate, and reference strain rate, respectively, with a value of 10^{-3}/s. The homogenization temperature is $T^* = (T_s\text{-}T_0)/(T_m\text{-}T_0)$, where T_m is the material melting point, T_s is the shear zone temperature, and the room temperature T_0 is 20 °C.

$$\begin{cases} A(HRC)= 0.3414(HRC)^2 - 12.13HRC + 487.1, \\ n(HRC) = -0.01331HRC + 0.7462. \end{cases} \tag{23}$$

In the inclined plane five-axis machining unit, the step distance, cutting depth, rotational speed, and feed rate were set as 1 mm, 1 mm, 500 r/min and 200 mm/min, respectively. The feed direction and cutter axis were changed evenly, and the corresponding three-way milling forces F_{cx}, F_{cy} and F_{cz} under the cutter coordinate system were calculated, as shown in Figure 7. The three figures together constitute the abstract static milling force database for the five-axis machining of curved surfaces in Figure 7.

In Figure 7, the database takes the characteristic sequence parameters κ_f and κ_a of the cutter axis as variables, and uniformly stores the three-way milling forces under different cutter axis vectors in the five-axis machining process. The sampling points in the database are based on the oblique plane five-axis machining, and have a mapping relationship with the cutter positions of the curved surface five-axis machining. The cutting force values in the database are derived from the established milling force prediction model of oblique plane five-axis machining. Obviously, once the cutter axis vector is determined, the three-way milling forces F_{cx}, F_{cy} and F_{cz} are all waveforms that change continuously with

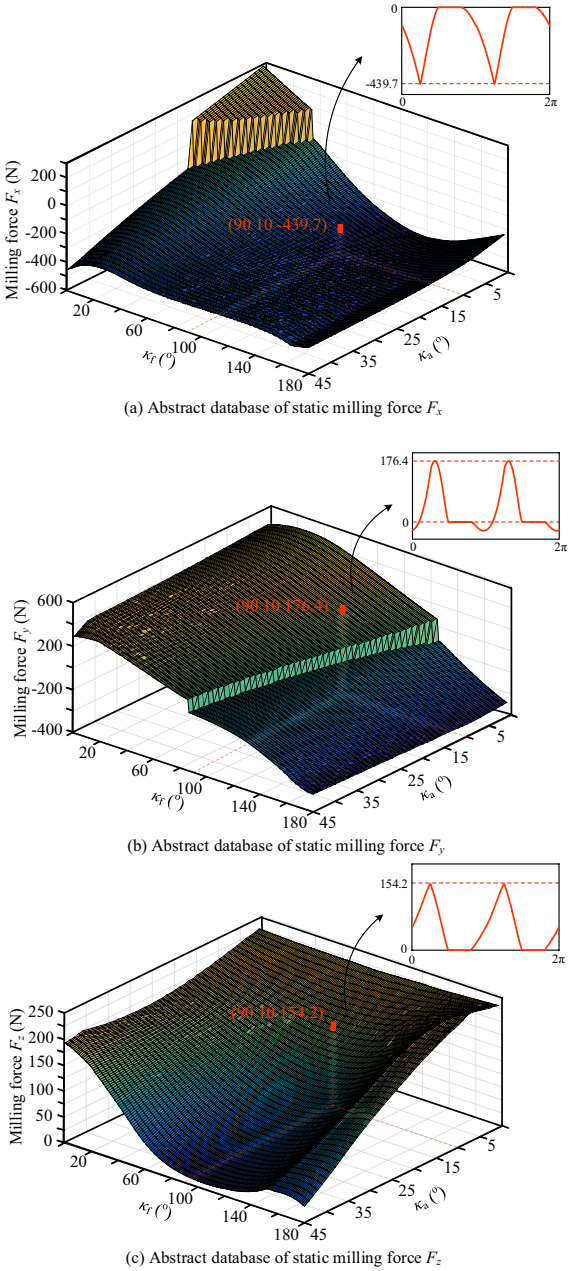

(a) Abstract database of static milling force F_x

(b) Abstract database of static milling force F_y

(c) Abstract database of static milling force F_z

Figure 7 Abstract static milling force database

the cutter rotation in the time domain. Although Figure 7 presents the peak value of the cutting force waveform, each sampling point corresponds to a complete periodic milling force of oblique plane five-axis machining. Taking point (90 10) as an example, the three-way periodic milling forces are shown in the upper right corner of Figure 7, and the peak values in the three directions are −439.7 N, 176.4 N, and 154.2 N, respectively. Clearly, the changes in the cutter axis and feed direction significantly affect the amplitude and direction of the milling force.

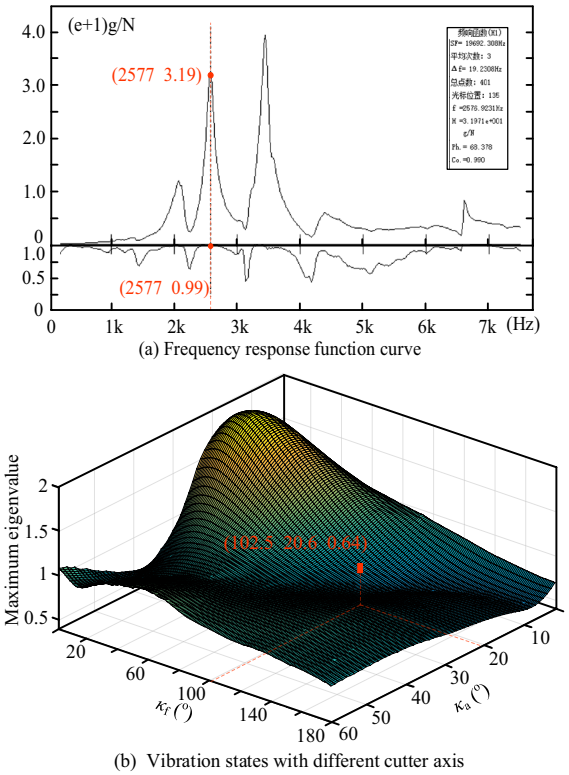

Figure 8 Abstract vibration state database

The milling forces F_{cx} and F_{cy} both decreased with the increase in the cutter dip angle and feed deflection angle. The milling force F_{cz} increased with the decrease in the cutter dip angle, and first decreased and then increased with the decrease in the feed deflection angle.

Similarly, for the inclined plane five-axis machining unit, the step distance, cutting depth, rotational speed, and feed rate are 0.3 mm, 0.4 mm, 9500 r/min, and 150 mm/min, respectively. Acceleration sensor and impact hammer were used to measure the amplitude-frequency curve and coherence curve of the frequency response function of the flexible cutter system, as shown in Figure 8(a). A large number of experiments show that the machining system is most sensitive to the second natural frequency, which is 2577 Hz, and the coherence is 0.99 close to 1. The damping ratio is 0.022 by using the complex mode single degree of freedom fitting method, and the stiffness is 1.905×10^4 N/mm by further combining with the amplitude-frequency curve. By changing the cutter axis and feed direction evenly, all the maximum eigenvalues of the transfer matrix under different combinations of characteristic parameters were calculated based on the derivation in Section 4.1. The obtained vibration state database in the abstract two-dimensional space is shown in Figure 8(b).

The research object in Figure 8 is the inclined plane five-axis machining unit that uniquely corresponds to each group of characteristic parameters, which reflects the stability of the cutter position on the tool path in curved surface five-axis machining. Taking point (103.5 20.6) as an example, the maximum eigenvalue of the transfer matrix of the former is less than 1; hence, the milling system is stable. Conversely, if the eigenvalue is greater than 1, then chatter will occur. The changes in the cutter axis and feed direction also influence the vibration state. Overall, chatter is more likely to occur under the combination of a small cutter dip angle and feed deflection angle; machining tends to be more stable under

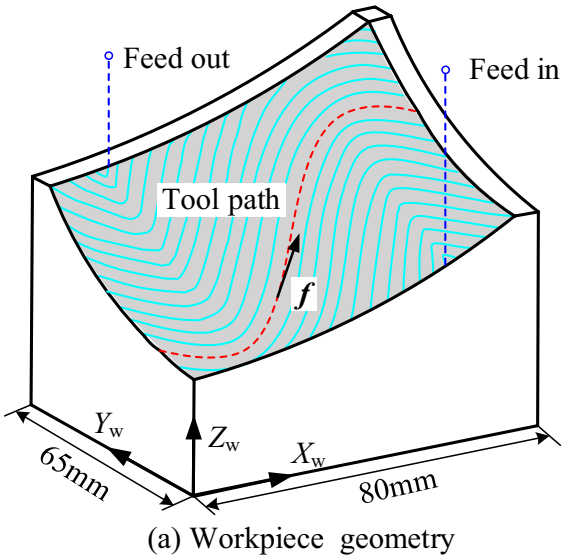

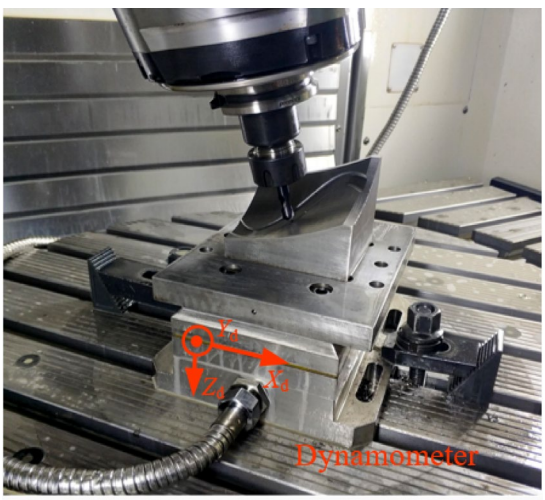

Figure 9 Milling force experiment of a curved surface

other combinations. This law has a positive correlation with the milling force because a larger force is more likely to cause chatter.

4.3 Verification Experiments

To further illustrate the convenience of the dynamics database based on dimension reduction and mapping, five-axis milling force and vibration state experiments on curved surfaces were conducted. Using the modeling and programming modules of Unigraphics NX software, the workpiece geometry and tool path with universal representation were designed. As shown in Figure 9(b), the experimental setup consists of a vertical five-axis CNC machining center. The ball-end mill, workpiece material, and machining parameters are described in Section 4.1.

The milling force experiment is shown in Figure 9. The tool path was sinusoidal, and the cutter axis was set to tilt forward 10° relative to the part. During the experiment, the milling force was synchronously measured using a dynamometer. Taking the tool path marked in red in Figure 9(a) as an example, the left side of Figure 10 shows the measured three-way milling force. Meanwhile, the sequence of characteristic parameters of the cutter position points were extracted, namely the feed deflection angle κ_f and cutter dip angle κ_a. From the established abstract milling force database shown in Figure 7, the force value under each group of characteristic parameters is determined. The tool path force can be predicted by uniformly transforming it into the dynamometer coordinate system. The results of the three-way milling force are shown on the right side of Figure 10.

The experimental results indicate that the predicted and measured three-way milling forces along the tool path follow the same trend, and the maximum amplitude and minimum amplitude are also in good agreement as a whole. The local maximum error is less than 20%, which is within a good acceptance range [4, 30]. The main reasons for the deviation include that the cutting edge curve is discrete into a series of independent straight edge oblique cutting, the cutter position point is approximately a micro-inclined plane, the limitation of the dynamic mechanical properties of the workpiece material, and the machining error and measurement error in the experimental process. At the same time, the tool path force prediction efficiency based on the abstract milling force database is extremely high because the simple and fast data search and extraction process takes almost zero time. In short, the experiment confirms the accuracy and efficiency of the milling force model with dimension reduction and mapping.

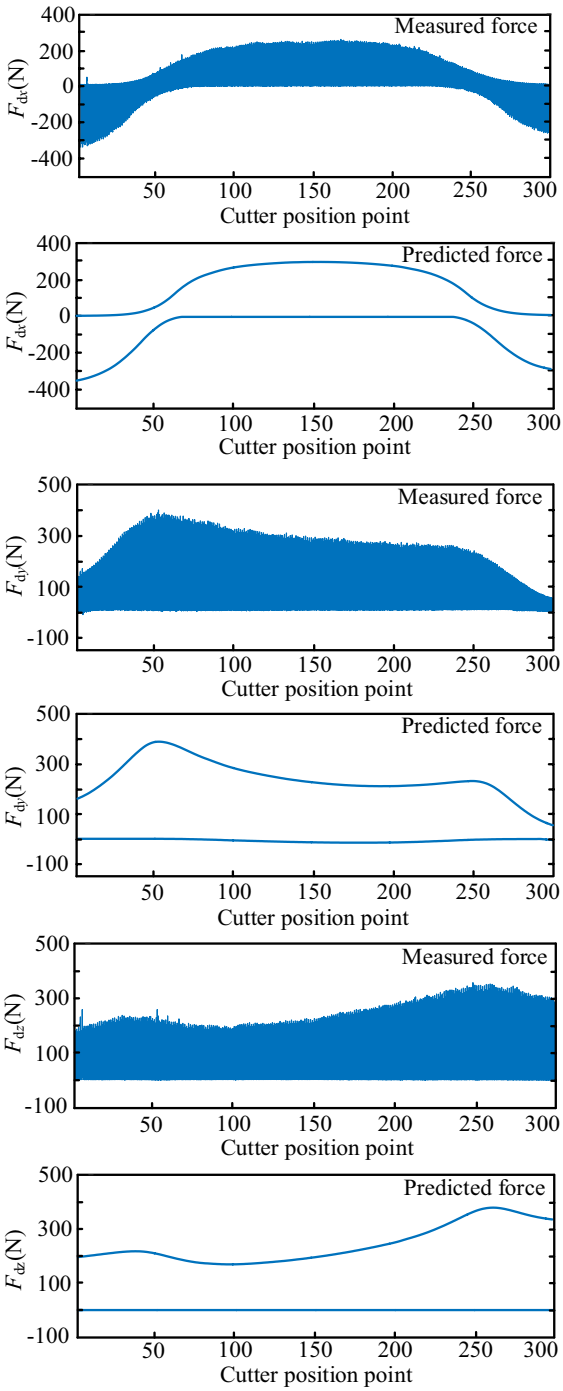

Figure 10 Measured and predicted milling force along tool path

The vibration experiment is shown in Figure 11. The tool path was generated by region driving. During the experiment, the vibration signal of the cutter system was measured synchronously by an acceleration sensor, while the vibration state was determined by spectrum analysis. Feed rate, step distance, cutter dip angle and

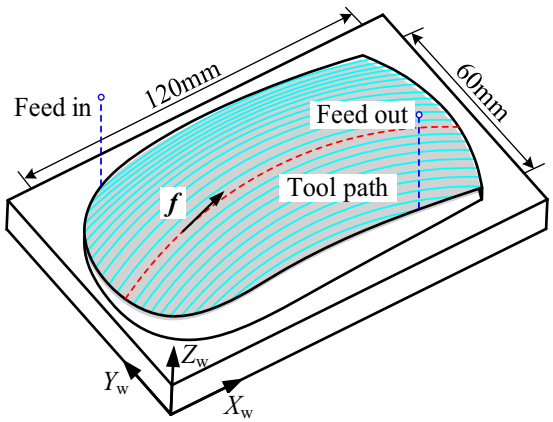

(a) Workpiece geometry

(b) Machining scene

Figure 11 Vibration state experiment of curved surface

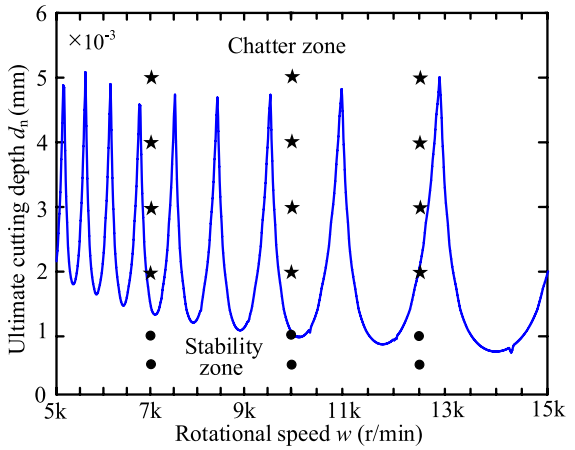

(a) Stability lobe diagram

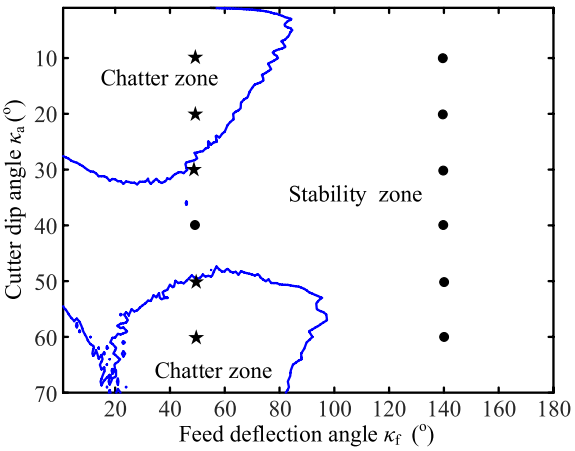

(2) Stability contour diagram

Figure 12 Chatter-stability cutting experiment range (star, chatter, filled circle, stability)

feed deflection angle were set to 150 mm/min, 0.4 mm, 10° and 90°, respectively. The stability lobe diagram of rotational speed and cutting depth was generated based on the theory of Section 4.1, as shown in Figure 12(a). With the change of rotational speed, the ultimate cutting depth shows a lobe shape. Machining experiments with rotational speeds of 7000, 10000 and 12500 r/min were carried out along the tool path, respectively. The theoretical prediction of vibration state was basically consistent with the experimental measurement when the cutting depth was changed in turn, as marked in Figure 12(a). The critical curve with transfer matrix characteristic 1 was extracted from the abstract vibration state database of Figure 8, as shown in Figure 12(b). Machining experiments with feed deflection angles of 50° and 140° were carried out along the tool path, and the theory and experiment were also in good agreement when the cutter dip angle was changed in turn, as marked in Figure 12(b).

Typical spectrum analysis results of vibration signals are shown in Figure 13. The amplitude near the natural frequency 2557 Hz in Figures 13(a), (b), (c) and (d) reached 1.77, 3.71, 6.64 and 11.09 g respectively, and the chatter phenomenon is obvious. Their eigenvalues in the vibration state database are 1.02, 1.18, 1.43 and 1.65 respectively, which are all greater than 1. Obviously, the larger the eigenvalue, the more obvious the chatter. Among them, the harmonic frequency is farther away from the chatter frequency ω_c and differs by several cutting frequencies ω_t, and the expression is $\omega_c+i\omega_t$ (i=±1, ±2, ...). Figure 13(e) represents stability machining with a frequency amplitude of 0.23 g. Its eigenvalue in the vibration state database is 0.81, which is less than 1. Therefore, the experiment demonstrates the accuracy of the vibration state database and the high chatter stability prediction efficiency based on dimension reduction and mapping.

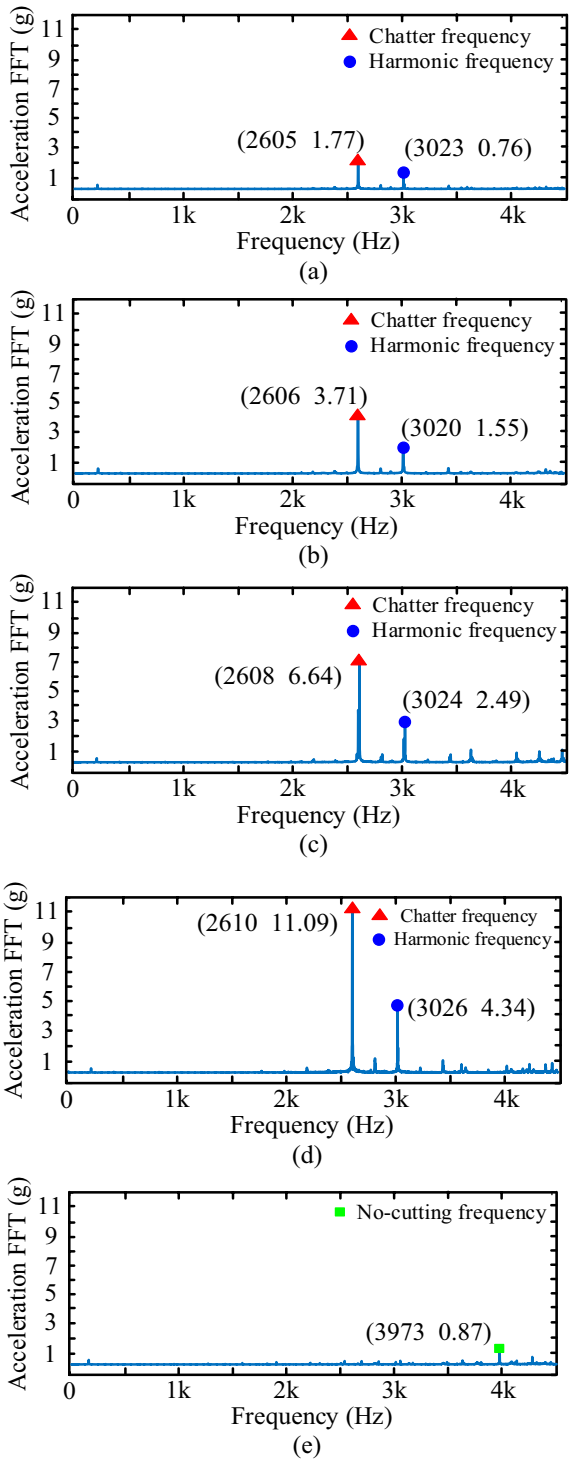

Figure 13 Frequency domain of the vibration signal measured

5 Conclusions

In this study, the differential discretization method was used to simplify each cutter position along the tool path in curved surface five-axis machining into tiny inclined plane five-axis machining, which reduces the research complexity.

(1) The spatial relationship between the feed, cutter, and workpiece was also well described. Furthermore, an abstract two-dimensional space with the feed deflection angle and cutter dip angle as base variables was constructed. The mapping relationship between the cutter position point and space point sets was established, and the dimension reduction expression of curved surface five-axis CNC machining was realized.

(2) The static milling force prediction model and the vibration state analysis model were established successively, taking the inclined plane five-axis machining as a research unit. Finally, the dynamics analysis results were uniformly stored in the abstract space to form a database, making the prediction process into a fast data extraction process.

(3) The measured vibration state and milling force in experiments were consistent with theoretical predictions, which proves the accuracy and high efficiency of the dynamics analysis model based on dimension reduction and mapping.

Acknowledgements
Not applicable.

Author Contributions
MG wrote the manuscript, planning and implementing the main research work of this paper; ZW and MW put forward the overall research idea and experimental platform; ZZ and SL assisted with English writing and verification experiments. All authors read and approved the final manuscript.

Authors' Information
Minglong Guo, born in 1989, is currently an associate researcher at *China Academy of Engineering Physics*, China. His main research interests are cutting mechanics and dynamics.
Zhaocheng Wei, born in 1981, is currently an associate professor at *Dalian University of Technology, China*. His main research interests are NC machining tools and processes.
Minjie Wang, born in 1958, is currently a professor at *Dalian University of Technology, China*. His main research interests are mold manufacturing technology and advanced processing technology.
Zhiwei Zhao, received his mater degree on mechanical engineering in *Dalian University of Technology, China*.
Shengxian Liu, is currently an associate engineer at *Engineering Training Centre of Dalian University of Technology, China*.

Funding
Supported by National Natural Science Foundation of China (Grant Nos. 52005078, U1908231, 52075076).

Data availability
If necessary, please contact the corresponding author.

Declarations

Competing Interests
The authors declare no competing financial interests.

Received: 8 November 2022 Revised: 25 September 2023 Accepted: 19 October 2023
Published online: 13 November 2023

References

[1] Z Li, Q Liu, S Yuan, et al. Prediction of dynamic cutting force and regenerative chatter stability in inserted cutters milling. *Chinese Journal of Mechanical Engineering*, 2013, 26(3): 555-563.
[2] M Fontaine, A Moufki, A Devillez, et al. Modelling of cutting forces in ball-end milling with tool-surface inclination: part I: predictive force model and experimental validation. *Journal of Materials Processing Technology*, 2007, 189(1-3): 73-84.
[3] Z Q Yao, X G Liang, L Luo, et al. A chatter free calibration method for determining cutter runout and cutting force coefficients in ball-end milling. *Journal of Materials Processing Technology*, 2013, 213(9): 1575-1587.
[4] M L Guo, Z C Wei, J Wang, et al. A new analytical ICCE and force prediction model for wide-row machining of free-form surface. *J. Mech. Sci. Technol.*, 2023, 37: 7-16.
[5] E Aras, A Albedah. Extracting cutter/workpiece engagements in five-axis milling using solid modeler. *Int. J. Adv. Manuf. Technol.*, 2014, 73(9-12): 1351-1362.
[6] Y Yang, W Zhang, M Wan, et al. A solid trimming method to extract cutter-workpiece engagement maps for multi-axis milling. *Int. J. Adv. Manuf. Technol.*, 2013, 68(9-12): 2801-2813.
[7] W Ferry, D Yip-Hoi. Cutter-workpiece engagement calculations by parallel slicing for five-axis flank milling of jet engine impellers. *J Manuf Sci E-T ASME*, 2008, 130(5): 383-392.
[8] Y Boz, H Erdim, I Lazoglu. Modeling cutting forces for 5-axis machining of sculptured surfaces. *Advanced Materials Research*, 2011, 223: 701-712.
[9] B K Fussell, R B Jerard, J G Hemmett, et al. Modeling of cutting geometry and forces for 5-axis sculptured surface machining. *Computer-Aided Design*, 2000, 35(4): 333-346.
[10] Z C Wei , M J Wang, J N Zhu, et al. Cutting force prediction in ball end milling of sculptured surface with Z-level contouring tool path. *Int. J. Mach. Tools Manuf.*, 2011, 51(5): 428-432.
[11] E Aras , H Y Feng. Vector model-based workpiece update in multi-axis milling by moving surface of revolution. *Int. J. Adv. Manuf. Technol.*, 2011, 52(9): 913-927.
[12] Y Sun, Q Guo. Numerical simulation and prediction of cutting forces in five-axis milling processes with cutter run-out. *Int. J Mach. Tools Manuf.*, 2011, 51(10-11): 806-815.
[13] X Zhang, J Zhang, B Pang, et al. An accurate prediction method of cutting forces in 5-axis flank milling of sculptured surface. *Int. J. Mach. Tools Manuf.*, 2015, 104: 26-36.
[14] M L Guo, Z C Wei, M J Wang, et al. Modal parameter identification of general cutter based on milling stability theory. *Journal of Intelligent Manufacturing*, 2020, (1): 221-235.
[15] D Bachrathy, G Stepan. Improved prediction of stability lobes with extended multi frequency solution. *CIRP Annals-Manufacturing Technology*, 2013, 62(1): 411-414.
[16] P V Bayly, J E Halley, B P Mann, et al. Stability of interrupted cutting by temporal finite element analysis. *J. Manuf. Sci. E-T. ASME*, 2003, 125(2): 220-225.
[17] T Insperger, G Stepan. Updated semi-discretization method for periodic delay-differential equations with discrete delay. *International Journal for Numerical Methods in Engineering*, 2004, 61(1): 117-141.
[18] Y B Dai, H K Li, Q Zhou, et al. Research on modeling method of machining stability in five-axis ball end milling based on enhanced complete discretization method. *Journal of Mechanical Engineering*, 2019, 55(23): 189-199. (in Chinese)
[19] M Li, G Zhang, Y Huang. Complete discretization scheme for milling stability prediction. *Nonlinear Dynamics*, 2013, 71(1-2): 187-199.
[20] Y B Dai, H K Li, H B Liu, et al. Dynamics and stability analysis of five-axis ball end milling with low radial immersion considering cutter runout. *J. Manuf. Process*, 2023, 92: 479-499.
[21] E Budak, L T Tunç, S Alan, et al. Prediction of workpiece dynamics and its effects on chatter stability in milling. *CIRP Annals-Manufacturing Technology*, 2012, 61(1): 339-342.
[22] O Ozkirimli, L T Tunc, E Budak. Generalized model for dynamics and stability of multi-axis milling with complex tool geometries. *Journal of Materials Processing Technology*, 2016, 238: 446-458.
[23] E Ozturk, E Budak. Dynamics and stability of five-axis ball-end milling. *J Manuf Sci E-T ASME*, 2010, 132(2): 021003-021003-13.
[24] M Wan, W H Zhang, G Tan, et al. New algorithm for calibration of instantaneous cutting-force coefficients and radial run-out parameters in flat end milling. *Proc. Inst. Mech. Eng., B J. Eng. Manuf.*, 2007, 221: 1007-1019.
[25] Z C Wei, M L Guo, M J Wang, et al. Prediction of cutting force for ball end mill in sculptured surface based on analytic model of CWE and ICCE. *Machining Science and Technology*, 2019, 23(5): 688-711.
[26] H H Zeng, X T Hu, D Yang. Analytical modeling of residual stresses in laser-assisted milling AerMet100 steel. *Optics and Laser Technology*, 2023, 158: 108931.
[27] M Wan, D Y Wen, W H Zang, et al. Prediction of cutting forces in flexible micro milling processes by considering the change of instantaneous cutting direction. *J. Manuf. Process*, 2023, 90: 180-195.
[28] R Chakrabarty, J Song. A modified Johnson-Cook material model with strain gradient plasticity consideration for numerical simulation of cold spray process. *Surface & Coatings Technology*, 2020, 397: 125981.
[29] G H Li. *Prediction of adiabatic shear in high speed machining based on linear pertubation analysis*. Dalian: Dalian University of Technology, 2009.
[30] S Makhfi, A Dorbane, F Harrou, et al. Prediction of cutting forces in hard turning process using machine learning methods: a case study. *J. Materi. Eng. and Perform*, 2023.